AMERICAN ACADEMY OF OPHTHALMOLOGY®

Censoring the Floor Effect in Long-Term Stargardt Disease Microperimetry Data Produces a Faster Rate of Decline

Jason Charng, PhD,[1,2] *Jennifer A. Thompson, PhD,*[3] *Rachael C. Heath Jeffery, MD,*[1,4] *Amy Kalantary, MD,*[1] *Tina M. Lamey, PhD,*[3] *Terri L. McLaren, BSc,*[1,3] *Fred K. Chen, PhD*[1,4,5,6]

Purpose: To evaluate progression rate estimation in long-term Stargardt disease microperimetry data by accounting for floor effect.

Design: Cohort study.

Subjects: Thirty-seven subjects (23 females, 14 males) with biallelic ABCA4 pathogenic or likely pathogenic variants and more than >2 years of longitudinal microperimetry data.

Methods: Cross-sectional and longitudinal microperimetry data (Grid A: 18° diameter, Grid B: 6° diameter; Macular Integrity Assessment microperimeter, dynamic range 0−36 decibels [dB]) was extracted from patients with biallelic mutation in the adenosine triphosphate-binding cassette subfamily A member 4 (*ABCA4*) gene. For each eye, mean sensitivity (MS) and responding point sensitivity (RPS) rates were extracted. Floor censored sensitivity (FCS) progression rate, which accounts for the floor effect at each locus by terminating calculation when scotoma was observed in 2 consecutive visits, was also calculated. In a subset of eyes with ≥1 scotomatous locus at baseline (Grid A), sensitivity progression of loci around the scotoma (edge of scotoma sensitivity [ESS]) was examined against other progression parameters. Paired *t* test compared progression rate parameters across the same eyes.

Main Outcome Measures: Microperimetry grid parameters at baseline and progression rates.

Results: A total of 37 subjects with biallelic *ABCA4* mutations and >2 years of longitudinal microperimetry data were included in the study. In Grid A, at baseline, the average MS and RPS were 16.5 ± 7.9 and 19.1 ± 5.7 dB, respectively. Similar MS (18.4 ± 7.6 dB) and RPS (20.0 ± 5.5 dB) values were found at baseline for Grid B. In Grid A, overall, MS, RPS, and FCS progression rates were −0.57 ± 1.05, −0.74 ± 1.24, and −1.26 ± 1.65 (all dB/year), respectively. Floor censored sensitivity progression rate was significantly greater than the MS or RPS progression rates. Similar findings were observed in Grid B (MS −1.22 ± 1.42, RPS −1.44 ± 1.44, FCS −2.16 ± 2.24, all dB/year), with paired *t* test again demonstrated that FCS had a significantly faster rate of decline than MS or RPS. In patients with progression data in both grids, MS, RPS, and FCS progression rates were significantly faster in the smaller Grid B. In 24 eyes with scotoma at baseline, fastest rate of decline was ESS combined with FCS compared with other progression parameters.

Conclusions: Incorporation of FCS can reduce confound of floor effect in perimetry analysis and can in turn detect a faster rate of decline.

Financial Disclosure(s): Proprietary or commercial disclosure may be found in the Footnotes and Disclosures at the end of this article. *Ophthalmology Science 2024;4:100581* *© 2024 by the American Academy of Ophthalmology. This is an open access article under the CC BY-NC-ND license (http://creativecommons.org/licenses/by-nc-nd/4.0/).*

Supplemental material available at www.ophthalmologyscience.org.

Stargardt disease (STGD1, Online Mendelian Inheritance in Man #248200) is the most common form of juvenile macular degeneration.[1,2] The pathophysiology of the disease involves impaired flippase activity of the adenosine triphosphate-binding cassette subfamily A member 4 (ABCA4) protein, resulting in the accumulation of bisretinoid fluorophores in the photoreceptor outer segments and lipofuscin-like fluorophores in the retinal pigment epithelium (RPE) which causes RPE and ultimately photoreceptor cell death.[3,4] Although there is no treatment for the disease, clinical trials are currently underway evaluating inhibitors of pathways implicated in the disease, including complement C5 (clinicaltrial.gov identifier NCT03364153), retinol binding protein 4 (NCT04489511, NCT05244304), RPE-specific 65 kDa protein (NCT03772665), vitamin A dimerization (identifier NCT04239625), as well as inducing autophagy (NCT04545736) or promoting lipofuscin removal (EudraCT 2018-001496-20).

© 2024 by the American Academy of Ophthalmology
This is an open access article under the CC BY-NC-ND license (http://creativecommons.org/licenses/by-nc-nd/4.0/). Published by Elsevier Inc.

https://doi.org/10.1016/j.xops.2024.100581
ISSN 2666-9145/24

Because of the predominant macular involvement in STGD1, characterization of the central retina is key in classifying the disease phenotype and essential for defining outcome measures in clinical trials. Recent studies have demonstrated the utility of measuring atrophy expansion rates for estimating disease progression in STGD1;[5,6] however, atrophy size does not correlate with function. Other proposed structure-based metrics of progression include rate of RPE loss via autofluorescence[7,8] as well as photoreceptor loss via OCT.[9] Again, it has been shown that functional abnormalities do not correlate with autofluorescence or OCT findings.[10] Microperimetry is commonly utilized to assess sensitivity to light in the central retina, with the ability to compensate for eye movements considered a key advantage over standard automated perimetry. The Macular Integrity Assessment (CenterVue) microperimeter is a confocal scanning laser ophthalmoscope-based device which has been extensively employed in clinical trials to assess retinal function.[11–13] Microperimetry progression can be determined by trend-based or event-based analysis of various parameters including average sensitivity across all loci in the test grid (i.e., mean sensitivity [MS]),[14–17] pointwise sensitivity,[18] sensitivity of subregions within the test grid,[19] and the number of scotomatous or nonscotomatous loci within the test grid.[16,20] Importantly, it has been shown that a faster sensitivity loss in trend-based analysis can be measured in eyes with geographic atrophy if average sensitivity across the test grid was calculated using only nonscotomatous loci (i.e., responding point sensitivity [RPS]) than MS. Furthermore, in eyes with STGD1, retinal sensitivity of loci bordering scotoma (i.e., edge of scotoma sensitivity [ESS]) declined faster than MS.[21,22] These findings are corroborated by a recent study in eyes with *USH2A* retinopathy that showed that ESS progression rate was significantly faster than both MS and RPS progression rates calculated in the same eye.[23] Although ESS has been shown to provide the fastest estimate of microperimetry progression rate in STGD1, not all eyes will present with a scotoma at baseline; hence, investigators cannot mark the scotoma boundary in order to select the ESS loci. Furthermore, retinal sensitivity measurement in eyes with severe vision loss due to STGD1 is confounded by the floor effect, consequent upon the highest luminance of the test stimulus set by the device. Assuming a linear sensitivity decline, a floor effect can underestimate the calculation of MS, RPS, and ESS rates as the "scotomatous" loci that do not progress further but are still included in the overall sensitivity estimates at each visit.

In this study, we explored trend-based analysis of long-term microperimetry data in STGD1. Importantly, we examined the utility of censoring the floor effect in pointwise progression analysis in estimating progression rates.

Methods

Ethics approval was obtained from the human ethics committee at the University of Western Australia (2021/ET000151) and Sir Charles Gairdner Hospital (RGS04985), Perth, Western Australia, Australia. Tenets of the Declaration of Helsinki were adhered to, and written informed consent was obtained from all participants for their data to be used for research purposes.

Patient Selection

The Western Australian Retinal Degeneration study database was interrogated for patients with biallelic mutations in the *ABCA4* gene and concurrent microperimetry data. Only patients with completed microperimetry tests were included.

Genetic Diagnosis

Targeted next-generation sequencing was performed on genomic DNA extracted from peripheral blood or saliva using a Stargardt/macular dystrophy panel (2014–2019 versions 1–5; 5–13 genes) or a retinal dystrophy next-generation sequencing SmartPanel (version 4 or 7; 183 or 233 genes),[24,25] which targeted all exons and flanking intronic regions of recognized macular or retinal dystrophy genes, as well as previously identified *ABCA4* deep-intronic variants. Sanger sequencing (Casey Eye Institute Molecular Diagnostics Laboratory or Molecular Vision Laboratory) confirmed candidate variants. Sequences were aligned to the *ABCA4* reference sequence NM_000350.2/3 (nucleotide 1, A of the start ATG), in accordance with Human Genome Variation Society recommendations version 15.11.[26] Sanger sequencing of the candidate disease-causing *ABCA4* variants was performed in parental or familial DNA to confirm biallelism. Variant pathogenicity was assessed and interpreted as per the American College of Medical Genetics and Genomics/Association for Molecular Pathology joint guidelines.[27]

Microperimetry Testing Protocol

Following pupil dilation (tropicamide 0.5% and phenylephrine 2.5%), microperimetry was conducted in a completely darkened room by trained ophthalmic assistants. Microperimetry testing was conducted using 2 grids (Fig S1, available at www.ophthalmologyscience.org). In instances where data from both grids were collected on the same day, a 2-minute break was given between tests. At baseline, all grids were manually shifted to match the fovea. Grid A pattern was based on the 10-2 pattern in the Humphrey Field Analyzer. Specifically, a 68-loci Cartesian array was arranged 1°, 3°, 5°, 7°, and 9° from the vertical or horizontal meridian to sample the central 18° diameter of the macula. Grid B assesses a smaller region of the central macula (6° diameter) and consists of 37 loci arranged in 3 concentric rings (radius 1°, 2°, and 3°) centered on the fovea. The centermost locus in Grid B was not analyzed as the fixation target provided during the testing interfered with its detection. In both grids, Goldmann III achromatic stimuli with a duration of 200 ms were presented on a dim white (1.27 cd/m^2) background using a 4-2 strategy. The differential dynamic range of the stimuli ranged from 0.08 to 317.04 cd/m^2 (36–0 decibels [dB]), with 0 dB indicating stimulus detection at the highest luminance. A scotomatous locus was defined as any locus that was not detected by the subject at the highest luminance and a −1 dB value was assigned, as per manufacturer data output.

Statistical Analysis

Microperimetry data from 1 eye only in each subject was included in the analysis. The eye with the longer longitudinal data in Grid A was chosen for analysis. The right eye was selected in instances of same follow-up period in both eyes. More importantly, only eyes with longitudinal data >2 years measured across ≥3 visits were included, with all subsequent tests performed using the

Table 2. Demographic, Clinical, and Variant Data of Patients with Biallelic *ABCA4* Mutation

ID	Sex	Age Onset	Study Eye	Age at 1st MAIA	BCVA at 1st MAIA	Grid A	Grid B	Anterior Eye	Allele 1	Allele 2
1	M	55	RE	56	0.00	Y	Y	Clear	c.4253 + 43G > A	c.[5177C > A; 5603A > T]
2	F	12	RE	14	0.86	Y	Y	Clear	c.4139C > T	c.[5461-10T > C;5603A > T]
3	F	27	LE	48	0.98	Y	N	Clear	c.2564G > A	c.3113C > T
4	M	62	RE	59	0.12	Y	N	Clear	c.2564G > A	c.3113C > T
5	M	82	RE	83	0.44	Y	N	IOL	c.2894A > G	c.5603A > T
6	F	76	RE	78	0.00	Y	Y	IOL	c.2894A > G	c.5603A > T
7	F	NA	RE	30	0.00	Y	Y	Clear	c.1805G > A	c.4577C > T[NT]
8	M	27	RE	30	1.32	Y	N	Clear	c.[3190 + 21A > G;4139C > T]	c.6079C > T
9	F	64	RE	65	1.08	Y	N	Mild NSC	c.71G > A	c.6204_6209delinsA
10	M	19	LE	25	0.90	Y	N	Clear	c.[2588G > C;5603A > T]	c.[5461-10T > C;5603A > T]
11	F	46	RE	49	0.00	Y	Y	Mild NSC	c.319C > T	c.3113C > T
12	F	17	LE	33	0.94	Y	N	Clear	c.3113C > T	c.4577C > T
13	F	9	RE	32	1.24	Y	N	Clear	c.3322C > T	c.3322C > T
14	M	21	RE	41	0.92	Y	N	Clear	c.[4222T > C;4918C > T]	c.5882G > A
15	M	18	RE	19	0.28	N	Y	Clear	c.[3523-9C > G;5882G > A]	c.4577C > T
16	F	19	RE	35	0.60	Y	N	Clear	c.[5461-10T > C;5603A > T]	c.6079C > T
17	F	72	RE	69	0.10	Y	Y	Mild NSC	c.[4222T > C;4918C > T]	c.5603A > T
18	M	16	RE	30	1.04	Y	N	Clear	c.768G > T	c.6079C > T
19	F	13	RE	46	1.36	Y	N	Clear	c.[67-1860A > G;6079C > T]	c.2966T > C
20	F	25	RE	34	0.82	Y	Y	Clear	c.3323G > T	c.5882G > A
21	F	NA	RE	32	−0.10	Y	Y	Clear	c.5603A > T	c.6088C > T
22	M	11	RE	11	0.32	N	Y	Clear	c.4320delT	c.[5461-10T > C;5603A > T]
23	M	30	LE	44	−0.06	Y	Y	Clear	c.3113C > T	c.[3608G > A;4537dup]
24	M	50	RE	54	0.44	Y	Y	Clear	c.5603A > T	c.6031_6044delinsAGTATTTAACCAATATTT
25	M	81	RE	82	0.70	Y	Y	Mild NSC	c.4577C > T	c.5603A > T
26	F	45	LE	58	0.04	Y	Y	Clear	c.[3237T > C;5603A > T]	c.[4670A > G;6148G > C]
27	F	32	RE	27	0.04	Y	Y	Clear	c.[2588G > C;5603A > T]	c.3322C > T
28	F	35	LE	56	0.06	Y	Y	Mild NSC	c.1957C > T	c.6089G > A
29	M	81	LE	82	0.34	N	Y	IOL	c.[2549A > G;4667+5G > T;5882G > A]	c.5603A > T
30	F	16	RE	25	0.92	Y	N	Clear	c.[5461-10T > C;5603A > T]	c.[4253 + 43G > A;4712T > A]
31	F	12	RE	19	0.80	Y	N	Clear	c.2626C > T	c.5714+5G > A
32	F	22	LE	26	0.04	Y	Y	Clear	c.768G > T	c.[5691G > T;5603A > T]
33	F	18	RE	22	0.22	Y	Y	Clear	c.768G > T	c.[5691G > T;5603A > T]
34	F	36	RE	56	−0.02	Y	Y	Clear	c.4577C > T	c.6079C > T
35	M	51	LE	53	0.10	Y	Y	Clear	c.4577C > T	c.6079C > T
36	F	29	RE	30	−0.08	Y	Y	Clear	c.1805G > A	c.4577C > T[NT]
37	M	46	RE	75	0.18	Y	Y	Mild NSC	c.4139C > T	c.5603A > T

ABCA4 = adenosine triphosphate-binding cassette subfamily A member 4; BCVA = best-correct visual acuity; F = female; IOL = intraocular lens; LE = left eye; M = male; MAIA = Macular Integrity Assessment; N = microperimetry data not available; NSC = nuclear sclerotic cataract; NT = not tested, presumed biallelic; RE = right eye; Y = microperimetry data available.

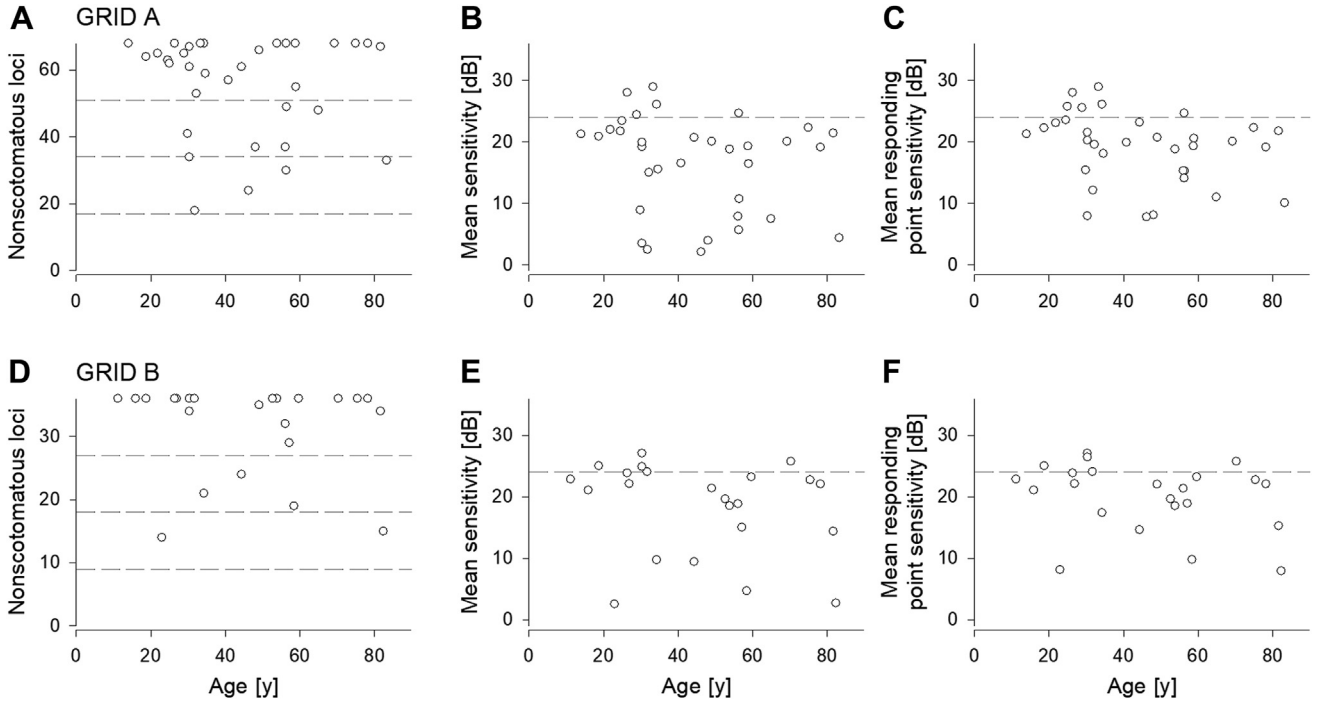

Figure 2. Baseline microperimetry data in STGD1 cohort. **A–C,** In Grid A, the number of seeing loci (**A**), MS (**B**), and RPS (**C**) at baseline are plotted against age, respectively. Gray dashed lines in Panel A divide the number of loci into quarters. Gray dashed lines in Panels B and D indicate the 24 dB cut-off for normal retinal function. **D–F,** In Grid B, the number of nonscotomatous loci (**D**), MS (**F**), and RPS (**G**) at baseline are plotted against age. Other details as per panels A to C. dB = decibels; MS = mean sensitivity; RPS = responding point sensitivity; STGD1 = Stargardt disease.

manufacturer's follow-up function to ensure that the same retinal loci were assessed over time.

Raw pointwise sensitivity values were extracted from each test. For each test, MS was calculated by taking an average of all sensitivity values across the entire grid. For each eye, MS values in Grid A or Grid B were plotted against time after initial visit and the gradient of the linear model was defined as overall MS progression rate. In RPS, any loci that were scotomatous at the first visit were excluded from analysis.[28] An average value was then calculated across the remaining loci to return RPS. Pointwise RPS progression rate was defined as the gradient of the linear fit when RPS was plotted against time after baseline, with mean RPS defined as the average of pointwise RPS progression rates. In floor censored sensitivity (FCS), at each locus, pointwise sensitivity values were included for analysis until the scotomatous value was recorded in 2 consecutive visits. For example, if sensitivity values at a locus were +15, +10, +5, −1, −1, and +2 dB chronologically across 6 visits, FCS will include sensitivity values from the first 5 visits (i.e., +15, +10, +5, −1, and −1 dB). Furthermore, the inclusion of the scotomatous values produced a greater average FCS progression rate than if these were excluded (sensitivity analysis, Table S1, available at www.ophthalmologyscience.org). Hence, whenever applicable, pointwise FCS progression rate included the first scotomatous value (i.e., the −1 dB measurement) in the linear regression. Mean FCS progression rate refers to the average of all pointwise FCS progression rates in the same eye.

A subanalysis was conducted in eyes with scotoma at baseline in Grid A. Specifically, MS, mean RPS, and mean FCS was calculated in these eyes. Additionally, ESS, defined as sensitivity of loci adjacent to any scotomatous locus, was also calculated.[23] We also examined progression rates when FCS was implemented in the ESS loci (i.e., mean ESS + FCS).

Unless otherwise stated, group data are summarized by average and standard deviation. Paired *t* test compared progression parameters across same eyes. A *P* value <0.05 was considered statistically significant. Statistical analysis was performed using R version 4.3.1 (R Foundation for Statistical Computing, https://www.r-project.org/).

Results

Patient Demographics

A total of 37 subjects (23 females, 14 males) with biallelic *ABCA4* pathogenic or likely pathogenic variants and >2 years of longitudinal microperimetry data (Table 2) were included. The average (range) age of symptom onset was 36 (9–82) years. At baseline microperimetry recording, the average (range) age was 44 (11–83) years and best-corrected visual acuity (logarithm of minimum angle of resolution, mean ± standard deviation) was 0.46 ± 0.46. Three eyes were pseudophakic and 6 had mild nuclear sclerosis. The remaining 28 eyes showed minimal lenticular changes.

Cross-Sectional Analysis

Grid A data were available from 34 eyes of 34 patients. At baseline, the mean number of nonscotomatous loci was

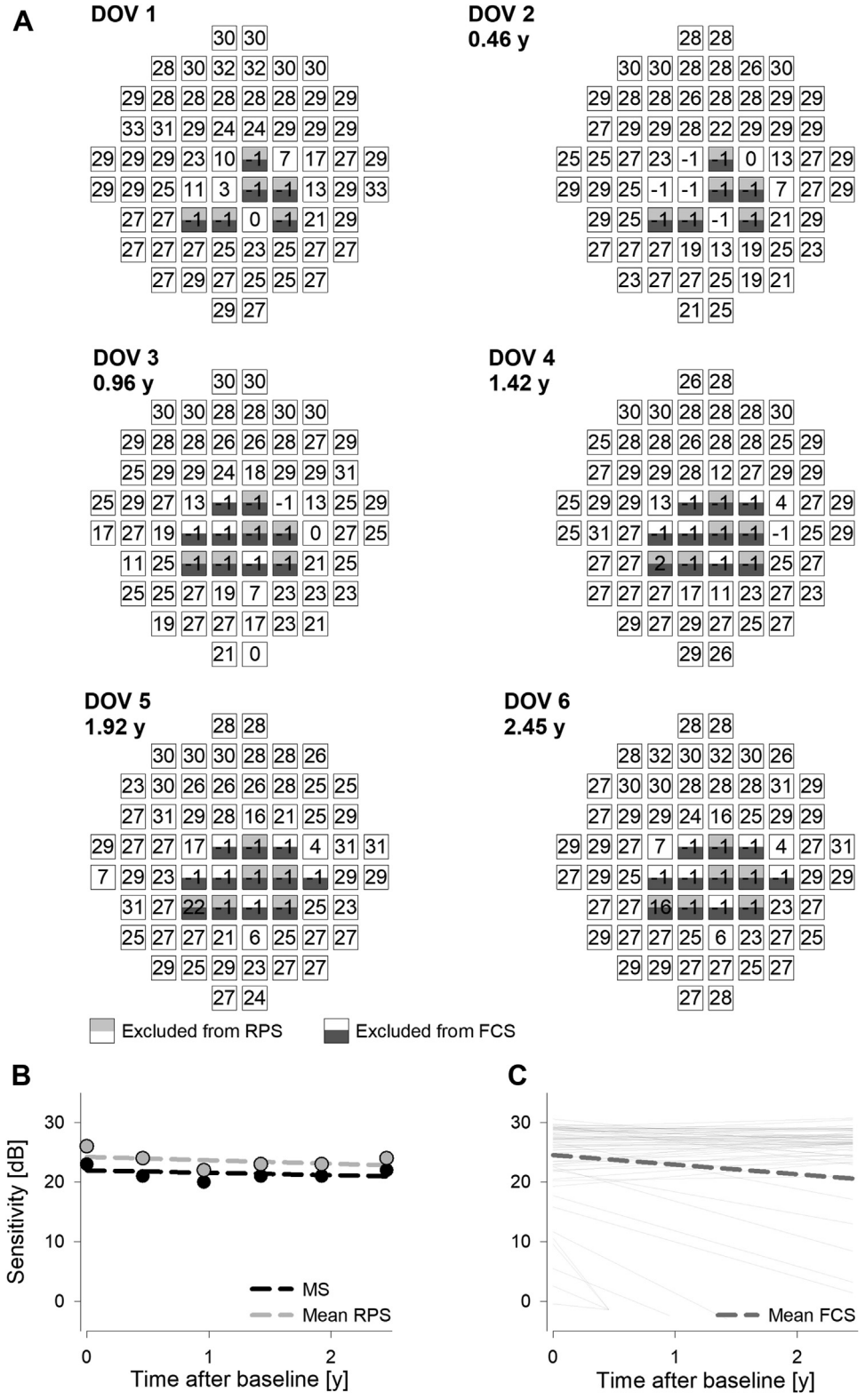

Figure 3. Derivation of FCS from a representative eye. **A,** Grid A sensitivity maps in an eye with biallelic *ABCA4* mutations over 6 visits. Squares with light gray shading on the top half indicate excluded from RPS calculations. Squares with dark gray shading on the bottom half indicate excluded from FCS calculations. **B,** Mean sensitivity (black filled) and RPS (gray filled) values plotted against time after baseline in the eye from Panel A. Dashed lines indicate linear fit. **C,** Floor censored sensitivity linear fit at each locus from Panel A is plotted as gray lines. Dashed thicker gray line indicates mean FCS rate from the individual FCS lines. *ABCA4* = adenosine triphosphate-binding cassette subfamily A member 4; dB = decibels; DOV = date of visit; FCS = floor censored sensitivity; MS = mean sensitivity; RPS = responding point sensitivity.

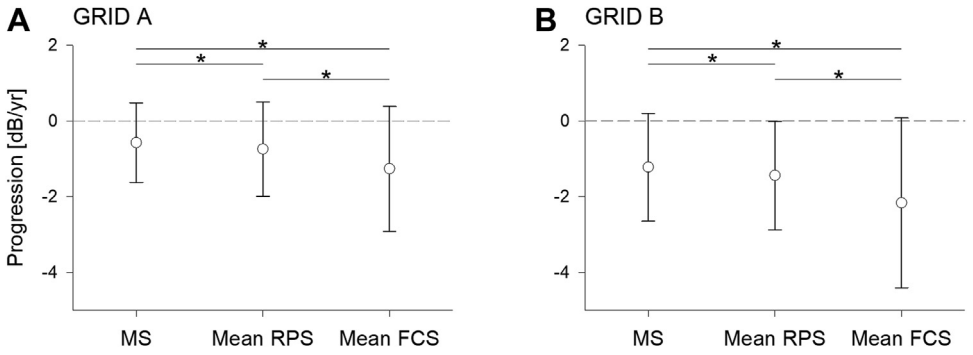

Figure 4. Comparing MS, mean RPS, and mean FCS rates. **A,** In Grid A, mean MS, mean RPS, and mean FCS rates are plotted. Error bars indicate standard deviation. * indicates significant difference from paired *t* test. **B,** Mean MS, mean RPS, and mean FCS are plotted from Grid B data. Other details as per panel **A**. FCS = floor censored sensitivity; MS = mean sensitivity; RPS = responding point sensitivity.

55.8 ± 15.0. Notably, 10 eyes showed measurable sensitivity across the entire grid and 5 additional eyes showed ≤3 scotomatous loci (Fig 2A). Across the cohort, the average MS and RPS were 16.5 ± 7.9 (Fig 2B) and 19.1 ± 5.7 (Fig 2C) dB, respectively. There was a weak association between the number of nonscotomatous loci ($y = -0.06x + 58.4$, $R^2 = 0.01$), MS ($y = -0.09x + 20.6$, $R^2 = 0.05$), and RPS ($y = -0.09x + 23.1$, $R^2 = 0.09$) with age.

In the smaller Grid B, the majority of eyes presented with no scotomas across the entire grid (13 of 23 eyes, mean nonscotomatous loci 31.5 ± 7.4, Fig 2D), and the average MS and RPS were 18.4 ± 7.6 (Fig 2E) and 20.0 ± 5.5 (Fig 2F) dB, respectively. Akin to Grid A, there was minimal association between the number of nonscotomatous loci ($y = -0.04x + 33.2$, $R^2 = 0.01$), MS ($y = -0.08x + 22.0$, $R^2 = 0.05$), and RPS ($y = -0.07x + 23.3$, $R^2 = 0.08$) with age.

Comparing FCS, MS, and RPS Progression Rates

In a patient with 6 Grid A recordings over 2.45 years (Fig 3A), by definition, 6 of 68 scotomatous loci were excluded from RPS and FCS analysis at baseline. Furthermore, FCS analysis for 4 loci was constrained to the third visit and 2 additional loci were restricted to the fourth and fifth visits, respectively. In this example, MS (including scotomatous loci at each visit; −1 dB) was calculated at each visit and the overall progression rate was −0.40 dB/year. Responding point sensitivity progression, derived at each visit by disregarding the 6 scotomatous loci at the first visit, demonstrated a faster rate of decline at −0.58 dB/year (Fig 3B). However, by taking the floor effect into consideration, FCS showed the greatest rate of decline at −1.61 dB/year (Fig 3C).

In all eyes with longitudinal Grid A data, overall, MS, mean RPS, and mean FCS progression rates were −0.57 ± 1.05 dB/year, −0.74 ± 1.24 dB/year, and −1.26 ± 1.65 dB/year, respectively (Fig 4A). Paired *t* test showed that the mean FCS progression rates were significantly greater than the MS or mean RPS progression rates. A subanalysis of eyes with scotoma at baseline in Grid A (n = 24, Table 3) showed MS had the lowest progression rate (−0.50 ± 0.78 dB/year) while the greatest rate of decline was observed in mean ESS + FCS (−3.59 ± 2.96 dB/year). Paired *t* tests revealed significant differences in progression rate between all parameters except for between FCS and ESS. In the smaller Grid B, paired *t* test again demonstrated that FCS showed a significantly faster rate of decline than MS or RPS (Fig 4B; MS −1.22 ± 1.42 dB/year, mean RPS −1.44 ± 1.44 dB/year, mean FCS −2.16 ± 2.24 dB/year).

In a subset of 20 patients with concurrent progression data in both grids, paired *t* test showed the rate of decline in all 3 progression parameters were significantly faster in the smaller Grid B than Grid A (MS, −1.26 ± 1.50 vs. −0.54 ± 1.15 dB/year; mean RPS, −1.44 ± 1.49 vs. −0.65 ± 1.18 dB/year; mean FCS −2.27 ± 2.36 vs. −1.29 ± 1.91; all $P < 0.05$).

Table 3. Subanalysis of 24 Eyes with Scotoma at Baseline in Grid A

	A Progression Rate [dB/yr]	Standard Deviation [dB/yr]
MS	−0.50	0.78
Mean RPS	−0.74	1.12
Mean FCS	−1.33	1.55
Mean ESS	−1.46	1.28
Mean ESS + FCS	−3.59	2.96

dB = decibels; ESS = edge of scotoma sensitivity; FCS = floor censored sensitivity; MS = mean sensitivity; RPS = responding point sensitivity.

Pointwise Progression Analysis

In Grid A, a subanalysis of loci (n = 439) that progressed to scotoma within each eye's observation period was conducted. Baseline retinal sensitivity was partitioned into 3 similar-sized bins (≤9 dB n = 153, 10−19 dB n = 135, ≥20 dB n = 151) and unpaired *t* tests showed that the progression rate in the lowest baseline sensitivity group (−2.6 ± 3.3 dB/year) was significantly lower than the mid (−6.4 ± 5.7 dB/year) and highest (−7.0 ± 2.2 dB/year) baseline sensitivity groups (Fig 5A). However, there was no statistical difference between the mid and the highest baseline sensitivity groups ($P = 0.48$).

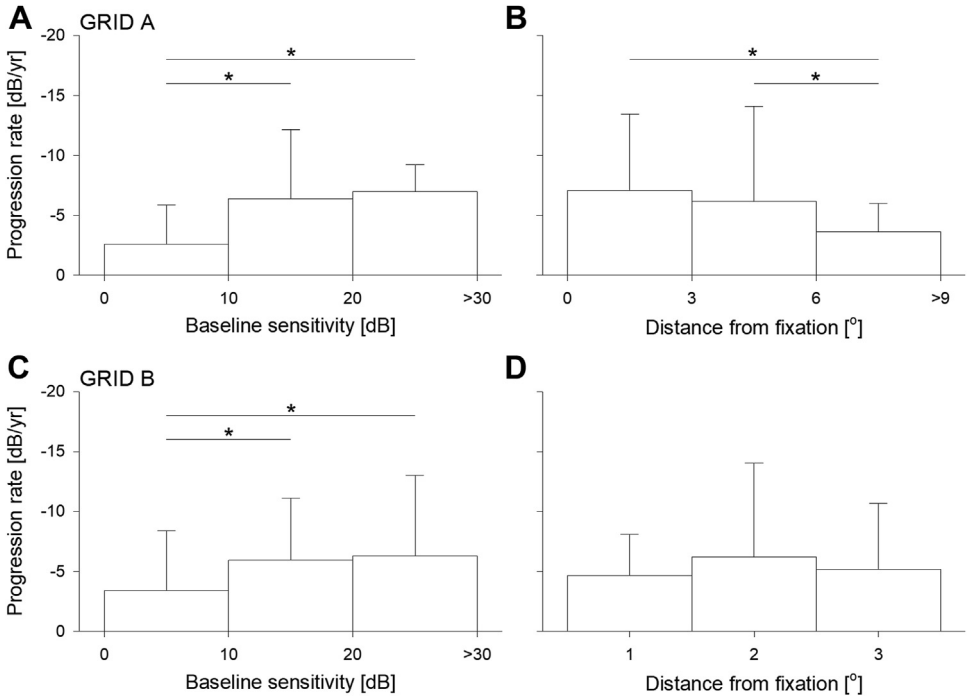

Figure 5. Pointwise analysis of loci that progressed to scotoma. **A, B,** In points that progressed to scotoma in Grid A, baseline sensitivities are divided into 3 bins (0–9, 10–19, >19 dB) and mean progression rate was plotted for each bin (**A**). Distance from progression are divided into 3 bins (0°–3°, 3°–6°, and 6°–9°) and mean progression rate plotted for each bin. Error bars indicate standard deviation. * indicates significant difference from unpaired *t* test. **C, D,** Mean progression rates for baseline sensitivity bins (**C**) and distance from fixation bins (**D**) are plotted from points that progressed to scotoma in Grid B. Note the smaller bin steps in panel D compared with panel B. Other details as per panel A. dB = decibels.

Perhaps not surprisingly, loci closer to the central fixation point tended to demonstrate a faster progression rate (Fig 5B) with unpaired *t* tests showing loci between 6° to 9° (−3.6 ± 2.4 dB/year, n = 133) had a significantly slower rate than those between 0° to 3° (−7.1 ± 6.4 dB/year, n = 44) and 3° to 6° (−6.2 ± 7.9 dB/year, n = 230).

There were fewer number of loci that progressed to scotoma in Grid B (n = 224). Similar to Grid A findings, loci in the lowest baseline sensitivity bin (Fig 5C, ≤9 dB, n = 61, −3.4 ± 5.0 dB/year) showed statically slower progression rates than those in 10 to 19 dB (n = 59, −5.9 ± 5.2 dB/year) and ≥20 dB (n = 104, −6.3 ± 6.7 dB/year) groups. There was no difference in progression rate between 10 and 19 dB and ≥20 dB groups (P = 0.71). Because of the smaller grid size, distance from fixation was partitioned into smaller step (1°) bins and showed no statistical difference between the 3 groups (Fig 5D, 1°, −4.6 ± 3.4 dB/year, n = 67; 2°, −6.2 ± 7.8 dB/year, n = 84; 3°, −5.2 ± 5.5 dB/year, n = 73).

Discussion

Appropriate, robust functional and structural outcome measures are key elements in STGD1 clinical trials. Studies have proposed anatomical markers from fundus autofluorescence[8,29] and OCT[21,30] as trial end points. Functionally, microperimetry has been commonly utilized to monitor localized changes in the disease. We showed that pointwise analysis combined with censoring of the floor effect produced a significantly faster estimation of rate of decline compared with the MS and RPS. Furthermore, progression rates appeared to be faster in loci with higher baseline sensitivity as well as further away from the fovea.

Mean sensitivity is a common microperimetry analysis parameter.[11–13] In the current study, the average MS of Grid A was 16.5 dB at baseline and MS progression rate was estimated −0.57 ± 1.05 dB/year, similar to the progression rate reported by a much larger cohort of patients with STGD1 (440 eyes, −0.87 dB/year) which employed the same grid pattern but on a different microperimetry device (Nidek MP-1).[31] The same authors showed, in a separate study, that the MS progression rate was −1.5 dB/year in a different cohort of STGD1 eyes but the progression rate of loci neighboring scotoma was significantly faster at −2.9 dB/year.[22] However, ESS calculation requires the presence of absolute scotoma at baseline, which was not detected in all eyes in our study (Grid A, 71%; Grid B, 43%). The previous study that reported higher ESS than MS progression rates showed a much higher percentage of eyes that had absolute scotoma at baseline (93%), which can be attributed to the more advanced disease stage in the previous study cohort as well as the difference in the highest stimulus luminance between the equipment used.

Given that not all eyes with STGD1 present with an absolute scotoma at baseline, we investigated analytical approaches that would detect a faster progression rate than MS. Responding point sensitivity, which only analyzed nonscotomatous loci at baseline which has been utilized in age-related macular degeneration,[28] *USH2A*-retinopathy,[23] and a previous STGD1[21] analyses, showed an overall significantly faster

rate than MS in our cohort (Grid A, −0.7 dB/year vs. −0.6 dB/year; Grid B, −1.4 dB/year vs. −1.2 dB/year). However, both MS and RPS incorporated scotomatous loci into the calculations, which in turn underestimated progression rate estimations. Indeed, in a cohort of 359 STGD1 eyes, a floor effect affecting MS calculation was evident in that overall MS progression was −0.68 dB/year but progression of only loci with baseline sensitivity >12 dB was much higher at −3.01 dB/year.[32] Hence, FCS was presented in the current study to reduce the effect of test loci reaching scotoma in longitudinal analysis. It is important to note that FCS reduces the floor effect but does not eliminate it, as the subanalysis of loci that progressed to scotoma demonstrated that loci with a baseline sensitivity <9 dB showed slower progression rates than those with higher baseline sensitivity. Furthermore, a sensitivity analysis demonstrated that the inclusion of the first scotomatous value in linear regression provided a significantly greater FCS decline rate than if the first scotomatous measurement was discarded. However, we note that the current FCS approach of including the first scotomatous value in the linear regression still underestimates the actual progression rate as the scotomatous value would have been reached before the patient's actual visit when the first scotomatous value was recorded. Our data suggest the rate of local sensitivity decline may accelerate as the edge of atrophy encroaches the test loci akin to a cliff edge effect.

The grid pattern used to assess STGD1 function is a key factor in designing future clinical trials. The smaller Grid B employed in the current study detected faster progression rate than Grid A in all 3 parameters assessed, which is not surprising due the centrifugal expansion of the disease from fovea. However, the potential drawback with a smaller test grid is the floor effect in a high proportion of loci in patients with advanced disease. On the other hand, a larger grid such as 10-2 may not have the spatial resolution to detect significant progression from baseline in a clinical trial with a fixed timeframe if MS was examined. Hence, customized grids assessing both parafoveal and perifoveal regions[33–35] combined with analytical approaches such as sectioning the grid into different retinal regions[22,36] combined with FCS may improve the likelihood of detecting statistically significant differences in progression rate in STGD1.

The strengths of the current study include analyzing relatively long follow-up data in patients with confirmed biallelic *ABCA4* variants. Furthermore, only data acquired with the follow-up function were included which ensured the same retinal locations were assessed at each time point. Although we were able to detect significant difference in progression rates between MS and FCS in our cohort, future studies examining FCS in a larger cohort with a greater genetic spectrum may demonstrate the usefulness of our FCS approach in stratifying patients into fast and slow progressors. A comparison of our trend-based FCS linear regression approach with the event-based approach of prespecifying a set threshold that a cluster of functional transition points need to reach will clarify the optimal number of testing sessions required in a clinical trial.

In conclusion, our data show that incorporating FCS in microperimetry analysis can reduce the floor effect when estimating progression rates in STGD1. This analytical approach can be performed in all patients irrespective of the test grid pattern. Floor censored sensitivity shows greater sensitivity to detect rates of decline than methods that incorporated all data points.

Footnotes and Disclosures

Originally received: April 22, 2024.
Final revision: July 2, 2024.
Accepted: July 15, 2024.
Available online: July 20, 2024. Manuscript no. XOPS-D-24-00123.

[1] Centre of Ophthalmology and Visual Science (incorporating Lions Eye Institute), The University of Western Australia, Perth, Western Australia, Australia.

[2] Discipline of Optometry, School of Allied Health, The University of Western Australia, Perth, Western Australia, Australia.

[3] Australian Inherited Retinal Disease Registry and DNA Bank, Department of Medical Technology and Physics, Sir Charles Gairdner Hospital, Perth, Western Australia, Australia.

[4] Royal Victorian Eye and Ear Hospital, Melbourne, Victoria, Australia.

[5] Ophthalmology, Department of Surgery, University of Melbourne, Melbourne, Victoria, Australia.

[6] Department of Ophthalmology, Royal Perth Hospital, Perth, Western Australia, Australia.

Disclosure(s):

All authors have completed and submitted the ICMJE disclosures form.

The author(s) have made the following disclosure(s):

Funded by the Telethon-Perth Children's Hospital Research Fund (F.K.C.), the Telethon grant (J.C., F.K.C.), the Miocevich Family grant (F.K.C.), the WA Health Near-miss Award (2021/GR000211, F.K.C.), the Australian National Health & Medical Research Council Career Development Fellowship (MRF1142962, F.K.C.), and the Australian National Health & Medical Research Council Centre of Research Excellence grant (GNT1116360, F.K.C.), Retina Australia (T.L.M., T.M.L., J.A.T.).

HUMAN SUBJECTS: Human subjects were included in this study. Ethics approval was obtained from the human ethics committee at the University of Western Australia (2021/ET000151) and Sir Charles Gairdner Hospital (RGS04985), Perth, Western Australia, Australia. Tenets of the Declaration of Helsinki were adhered to, and written informed consent was obtained from all participants for their data to be used for research purposes.

No animal subjects were used in this study.

Author Contributions:

Conception and design: Charng, Chen

Data collection: Charng, Thompson, Heath Jeffery, Kalantary, Lamey, McLaren, Chen

Analysis and interpretation: Charng, Thompson, Lamey, McLaren, Chen

Obtained funding: Chen

Overall responsibility: Charng, Thompson, Heath Jeffery, Kalantary, Lamey, McLaren, Chen

Abbreviations and Acronyms:

ABCA4 = adenosine triphosphate-binding cassette subfamily A member 4; **dB** = decibels; **ESS** = edge of scotoma sensitivity; **FCS** = floor censored

sensitivity; **MS** = mean sensitivity; **RPE** = retinal pigment epithelium; **RPS** = responding point sensitivity; **STGD1** = Stargardt disease.

Keywords:
ABCA4, Floor effect, Microperimetry, Progression, Stargardt disease.

Correspondence:
Fred K. Chen, PhD, Lions Eye Institute, 2 Verdun Street, Perth, Western Australia 6009, Australia. E-mail: fredchen@lei.org.au.

References

1. Heath Jeffery RC, Mukhtar SA, McAllister IL, et al. Inherited retinal diseases are the most common cause of blindness in the working-age population in Australia. *Ophthalmic Genet*. 2021;42(4):431−439.
2. Strauss RW, Ho A, Munoz B, et al. The natural history of the progression of atrophy secondary to Stargardt disease (ProgStar) studies: design and baseline characteristics: ProgStar Report No. 1. *Ophthalmology*. 2016;123(4):817−828.
3. Lenis TL, Hu J, Ng SY, et al. Expression of ABCA4 in the retinal pigment epithelium and its implications for Stargardt macular degeneration. *Proc Natl Acad Sci USA*. 2018;115(47):E11120−E11127.
4. Tsybovsky Y, Molday RS, Palczewski K. The ATP-binding cassette transporter ABCA4: structural and functional properties and role in retinal disease. *Adv Exp Med Biol*. 2010;703:105−125.
5. Heath Jeffery RC, Thompson JA, Lo J, et al. Genotype-specific lesion growth rates in Stargardt disease. *Genes*. 2021;12(12):1981.
6. Heath Jeffery RC, Thompson JA, Lo J, et al. Atrophy expansion rates in Stargardt disease using ultra-widefield fundus autofluorescence. *Ophthalmol Sci*. 2021;1(1):100005.
7. Muller PL, Pfau M, Mauschitz MM, et al. Comparison of green versus blue fundus autofluorescence in ABCA4-related retinopathy. *Transl Vis Sci Technol*. 2018;7(5):13.
8. Strauss RW, Kong X, Ho A, et al. Progression of Stargardt disease as determined by fundus autofluorescence over a 12-month period: ProgStar report no. 11. *JAMA Ophthalmol*. 2019;137(10):1134−1145.
9. Pfau M, Cukras CA, Huryn LA, et al. Photoreceptor degeneration in ABCA4-associated retinopathy and its genetic correlates. *JCI Insight*. 2022;7(2):e155373.
10. Sunness JS, Ifrah A, Wolf R, et al. Abnormal visual function outside the area of atrophy defined by short-wavelength fundus autofluorescence in Stargardt disease. *Invest Ophthalmol Vis Sci*. 2020;61(4):36.
11. Chew EY, Clemons TE, Jaffe GJ, et al. Effect of ciliary neurotrophic factor on retinal neurodegeneration in patients with macular telangiectasia type 2: a randomized clinical trial. *Ophthalmology*. 2019;126(4):540−549.
12. Kodjikian L, Creuzot-Garcher C, Korobelnik JF, et al. Microperimetry to predict disease progression in eyes at high risk of age-related macular degeneration disease: the PREVISION study. *Acta Ophthalmol*. 2023;101(2):e135−e142.
13. Lam BL, Davis JL, Gregori NZ, et al. Choroideremia gene therapy phase 2 clinical trial: 24-month results. *Am J Ophthalmol*. 2019;197:65−73.
14. Chew AL, Sampson DM, Chelva E, et al. Perifoveal interdigitation zone loss in hydroxychloroquine toxicity leads to subclinical bull's eye lesion appearance on near-infrared reflectance imaging. *Doc Ophthalmol*. 2018;136(1):57−68.
15. Hagag AM, Mitsios A, Gill JS, et al. Characterisation of microvascular abnormalities using OCT angiography in patients with biallelic variants in USH2A and MYO7A. *Br J Ophthalmol*. 2020;104(4):480−486.
16. Roshandel D, Thompson JA, Charng J, et al. Exploring microperimetry and autofluorescence endpoints for monitoring disease progression in PRPF31-associated retinopathy. *Ophthalmic Genet*. 2021;42(1):1−14.
17. Welker SG, Pfau M, Heinemann M, et al. Retest reliability of mesopic and dark-adapted microperimetry in patients with intermediate age-related macular degeneration and age-matched controls. *Invest Ophthalmol Vis Sci*. 2018;59(4):AMD152−A159.
18. Charng J, Sanfilippo PG, Attia MS, et al. Interpreting MAIA microperimetry using age- and retinal loci-specific reference thresholds. *Transl Vis Sci Technol*. 2020;9(7):19.
19. Chen FK, Patel PJ, Webster AR, et al. Nidek MP1 is able to detect subtle decline in function in inherited and age-related atrophic macular disease with stable visual acuity. *Retina*. 2011;31(2):371−379.
20. Schonbach EM, Wolfson Y, Strauss RW, et al. Macular sensitivity measured with microperimetry in Stargardt disease in the progression of atrophy secondary to Stargardt disease (ProgStar) study: report No. 7. *JAMA Ophthalmol*. 2017;135(7):696−703.
21. Pfau M, Huryn LA, Boyle MP, et al. Natural history of visual dysfunction in ABCA4 retinopathy and its genetic correlates. *Am J Ophthalmol*. 2023;253:224−232.
22. Schonbach EM, Strauss RW, Ibrahim MA, et al. Faster sensitivity loss around dense scotomas than for overall macular sensitivity in Stargardt disease: ProgStar report no. 14. *Am J Ophthalmol*. 2020;216:219−225.
23. Charng J, Lamey TM, Thompson JA, et al. Edge of scotoma sensitivity as a microperimetry clinical trial end point in USH2A retinopathy. *Transl Vis Sci Technol*. 2020;9(10):9.
24. Chiang JP, Lamey T, McLaren T, et al. Progress and prospects of next-generation sequencing testing for inherited retinal dystrophy. *Expert Rev Mol Diagn*. 2015;15(10):1269−1275.
25. De Roach J, McLaren T, Thompson JA, et al. The Australian inherited retinal disease registry and DNA bank. *Tasman Med J*. 2020;2(3):60−67.
26. den Dunnen JT, Dalgleish R, Maglott DR, et al. HGVS Recommendations for the description of sequence variants: 2016 update. *Hum Mutat*. 2016;37(6):564−569.
27. Richards S, Aziz N, Bale S, et al. Standards and guidelines for the interpretation of sequence variants: a joint consensus recommendation of the American College of medical genetics and genomics and the association for molecular Pathology. *Genet Med*. 2015;17(5):405−424.
28. Meleth AD, Mettu P, Agron E, et al. Changes in retinal sensitivity in geographic atrophy progression as measured by microperimetry. *Invest Ophthalmol Vis Sci*. 2011;52(2):1119−1126.
29. Charng J, Xiao D, Mehdizadeh M, et al. Deep learning segmentation of hyperautofluorescent fleck lesions in Stargardt disease. *Sci Rep*. 2020;10(1):16491.

30. Kong X, Ho A, Munoz B, et al. Reproducibility of measurements of retinal structural parameters using optical coherence tomography in Stargardt disease. *Transl Vis Sci Technol*. 2019;8(3):46.
31. Schonbach EM, Janeschitz-Kriegl L, Strauss RW, et al. The progression of Stargardt disease using volumetric hill of vision analyses over 24 months: ProgStar report no.15. *Am J Ophthalmol*. 2021;230:123−133.
32. Schonbach EM, Strauss RW, Munoz B, et al. Longitudinal microperimetric changes of macular sensitivity in Stargardt disease after 12 months: ProgStar report no. 13. *JAMA Ophthalmol*. 2020;138(7):772−779.
33. Dhooge PPA, Moller PT, Boon CJF, et al. The STArgardt Remofuscin Treatment Trial (STARTT): design and baseline characteristics of enrolled Stargardt patients. *Open Res Eur*. 2021;1:96.
34. Tanna P, Georgiou M, Aboshiha J, et al. Cross-sectional and longitudinal assessment of retinal sensitivity in patients with childhood-onset Stargardt disease. *Transl Vis Sci Technol*. 2018;7(6):10.
35. Testa F, Melillo P, Di Iorio V, et al. Macular function and morphologic features in juvenile stargardt disease: longitudinal study. *Ophthalmology*. 2014;121(12):2399−2405.
36. Kong X, Ibrahim-Ahmed M, Bittencourt MG, et al. Longitudinal changes in scotopic and mesopic macular function as assessed with microperimetry in patients with Stargardt disease: SMART study report no. 2. *Am J Ophthalmol*. 2022;236:32−44.